J Neurophysiol 98: 730–743, 2007.
First published April 25, 2007; doi:10.1152/jn.00457.2006.

Postural Responses Evoked by Platform Pertubations Are Dominated by Continuous Feedback

Herman van der Kooij[1] and Erwin de Vlugt[2]

[1]*Institute for Biomedical Technology, Department of Biomechanical Engineering, University of Twente, Enschede; and* [2]*Biomechanical Engineering, Neuromuscular Control Laboratory, Department of Mechanical Engineering, Delft University of Technology, Delft, The Netherlands*

Submitted 1 May 2006; accepted in final form 24 April 2007

van der Kooij H, de Vlugt E. Postural responses evoked by platform pertubations are dominated by continuous feedback. *J Neurophysiol* 98: 730–743, 2007. First published April 25, 2007; doi:10.1152/jn.00457.2006. Is human balance control dominated by time invariant continuous feedback mechanisms or do noncontinuous mechanisms play a significant role like intermittent control? The goal of this paper is to quantify how much of the postural responses evoked by pseudorandom external periodic perturbations can be explained by continuous time invariant feedback control. Nine healthy subjects participated in this study. Center of mass and ankle torque responses were elicited by periodic platform perturbations in forward-backward directions containing energy in the 0.06- to 4.5-Hz frequency band. Subjects had their eyes open (EO) or eyes closed (EC). Responses were decomposed into a periodic component and a remnant (stochastic) component using spectral analysis. It is concluded that periodic responses can explain most of the evoked responses, although the remnant power spectral densities (PSDs) were significant especially for slow responses ($<$0.2 Hz) and largest for EC. The found remnant PSD did depend on the sensory condition but not on the platform perturbation amplitude. The ratio of the body sway and ankle torque remnant PSD reflects the body dynamics. Both findings are consistent with the idea that estimation of body orientation is part of a continuous feedback loop and that (stochastic) estimation errors increase when one source of sensory information is removed. The findings are not consistent with the idea that discrete or discontinuous intermittent feedback mechanisms significantly shape postural responses.

INTRODUCTION

Upright standing requires corrective joint torques to resist the gravitational forces. How humans control corrective torques is a topic of long debate. Many researchers, especially those who are involved in modeling, consider balance control as a process in which body sway is continuously fed back (Alexandrov et al. 2005; Johansson et al. 1988; Kiemel et al. 2005; Park et al. 2004; Peterka 2000, 2003). According to this view, the postural control system has been considered a linear time-invariant (LTI) continuous feedback mechanism for stationary conditions. LTI feedback models exist in varying degrees of complexity. The simplest ones consist of a feedback gain matrix (Barin 1989; Park et al. 2004), eventually extended with time delays (Alexandrov et al. 2005; Peterka 2002). In those models, it is assumed that body orientation is perfectly known. Because no noise sources also are explicitly modeled, these models are deterministic. In other models, sensory integration was also incorporated in the feedback loop (Carver et al. 2005; Kiemel et al. 2005; Mergner et al. 2003; van der Kooij et al. 1999). These models postulate that the perception of body in space is imperfect and that estimation errors increase when sensory information is reduced (van der Kooij et al. 1999). The estimation dynamics also explain why humans sway very slowly when instructed to stand still (Kiemel et al. 2002). In other models, these slow dynamics of spontaneous postural sway are attributed to an external source outside the feedback loop being low-pass filtered white noise injected in the feedback loop at the output (Peterka 2000) or at the input (Dijkstra 2000). In the former case, the nature of the noise can be a mechanical disturbance caused by the hemodynamics due to heartbeats and by spirodynamics due to respiration. In the latter case, the noise can be considered as sensor noise or as fluctuations in the set point of the feedback loop. Low-pass filtered sensor noise in a model without state estimation is to some extent equivalent with a model with noisy state estimation with the difference that the slow dynamics itself are outside instead of inside the feedback loop. Note that in case sensor noise or stochastic processes are modeled, such as aforementioned internal mechanical perturbations, the LTI continuous feedback models are not deterministic anymore.

Other researchers advocated alternative stabilizing mechanisms by distinguishing an "open-loop" region, i.e., a region without feedback, and a "closed-loop" region characterized by feedback (Collins and De Luca 1993). This can be considered as intermittent control that has been postulated to be responsible for the slow dynamics of spontaneous postural sway (Bottaro et al. 2005). Others postulate that the balancing process is characterized by bias muscle adjustments that are considered as a sign of intermittent alterations in neural output (Lakie and Loram 2006; Loram et al. 2006). On average, the unidirectional bias adjustments occurred at intervals of ~400 ms and were considered as an "intrinsic constraint of the neuromuscular system." The fundamental difference of the proposed alternative stabilizing mechanisms from the continuous feedback models is that the former are discontinuous.

It has been argued that feedback alone is not sufficient to stabilize posture and that feed forward control might be involved also (Fitzpatrick et al. 1996; Gatev et al. 1999). In the formal definition of feed forward control, the control variable (e.g., muscle activation or joint torque) is independent from the controlled variable (e.g., body sway). From this definition, it

Address for reprint requests and other correspondence: H. van der Kooij, Biomechanical Engineering, University of Twente, PO Box 217, 7500AE Enschede, The Netherlands. (E-mail: h.vanderkooij@utwente.nl).

The costs of publication of this article were defrayed in part by the payment of page charges. The article must therefore be hereby marked "*advertisement*" in accordance with 18 U.S.C. Section 1734 solely to indicate this fact.

implies that feed forward control in principal never can warrant stabilization. In the discussion section, we will explain that "feed forward control" has been used in a way that is not in agreement with its formal definition. Feed forward control has been used to describe adaptation, disturbance compensation, and phase advances, which all can be considered as (adaptive) feedback control.

When a periodic stimulus is applied to a physiological system, the response is not only periodic but also contains nonperiodic components that are indicated as the remnant. Remnants can be due to the following. *1*) Nonlinearities of the perturbed system. Nonlinearities not only cause periodic responses at even and odd harmonics of the excited frequencies but also nonlinear stochastic distortions that look like noise (Pintelon and Schoukens 2001). As will be explained later intermittent controllers can be modeled with dead-zones or zero-order holds, which are static nonlinear elements. *2*) Time variant system behavior. Therefore the responses to periodic perturbations can vary in time, which will add a nonperiodic component in case the variation in time itself is no periodic but a stochastic process. *3*) Unmeasured stochastic sources that enters the feedback at the input (v in Fig. 1) or at the output (w in Fig. 1). As explained earlier for balance control, input noise corresponds with sensory or motor command noise and output noise with stochastic mechanical perturbations caused by hemodynamics or by spirodynamics. *4*) Measurement noise. In balance control, the center of mass (CoM) is often used to characterize body sway and the center of pressure (CoP), or ankle torque, to characterize control effort. CoM and CoP can be affected by measurement noise. Especially the CoM is difficult to asses because many assumptions are mostly required for calculation. In addition, skin movements introduce errors affecting the registration of anatomical landmarks that are necessary for calculation the CoM of each body segment.

The goal of this paper is to investigate whether the periodic components and the remnants of responses evoked by pseudo random periodic platform perturbations are consistent with continuous feedback control or otherwise with alternative concepts of balance control as proposed by others.

From the periodic body sway and ankle torque responses, frequency response functions (FRFs) of the stabilizing balance mechanism were estimated. To localize the stochastic source, we analyzed the correlation and ratio between body sway and ankle torque remnants. The sensitivity of the estimated stabilizing mechanisms and of the remnants to perturbation amplitude and visual condition were determined. The remnants were compared with ankle torque and body sway in quiet standing to test whether the remnants could be considered as a baseline of spontaneous activity. To investigate whether experimental observations are consistent with existing concepts of balance control introduced earlier, the predictions of different models were qualitatively compared with the experimentally estimated remnants and periodic responses.

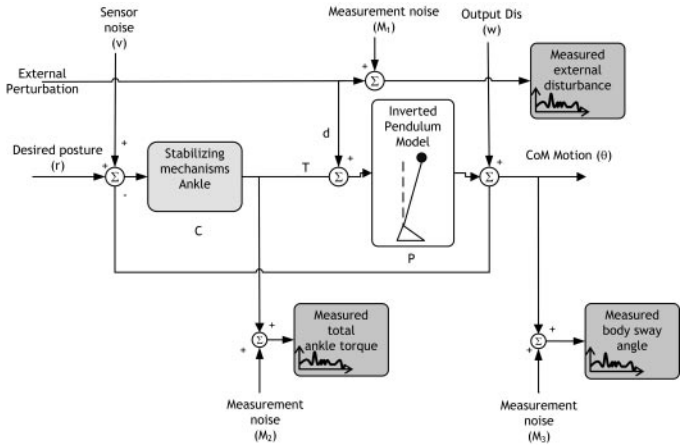

FIG. 1. A simple model of balance control.

METHODS

Method

The CoM and ankle torque recordings have been divided into periodic and nonperiodic (remnant) components. The ratio of the nonperiodic and period parts, as defined by the noise-to-signal ratio (NSR), indicates to what extent ankle torque is controlled by a deterministic LTI system. A small NSR value indicates the system is predominantly linear, time invariant, and without noise, whereas a large value indicates to nonlinear distortions or to the presence of noise. The deterministic LTI part is obtained from frequency response functions (FRFs) describing the dynamic behavior in the frequency domain, in this case from body sway to ankle torque [indicated by $C(\omega)$ in Fig. 1]. Finally, the remnants were analyzed to determine whether the remnants originate from external measurement noise or from noise injected into the feedback loop, whether the remnants are evoked by the perturbations or can be considered as a baseline of spontaneous activity with a similar power spectral density as observed during quiet standing, and at what location the noise enters the feedback loop in case the remnants originate from noise injected into the feedback loop.

Experiments

SUBJECTS. Nine subjects (age: 21 ± 1 yr, 6 males, 3 females) participated voluntarily in the experiment. All participants were healthy and did not suffer from any motor impairments or movement-related disorders. The protocol was approved by the local medical ethical committee and conformed to the principles of the Declaration of Helsinki. All participants gave their written informed consent prior to the experiment.

APPARATUS AND RECORDINGS. The participants stood with their arms folded in front of their chest on a force plate, embedded in a computer controlled 6° of freedom Stewart motion platform[1] (Hydraudyne HSE-6-MS-8-L-2D). Their feet were placed with the medial sides and the heels against a fixed foot frame resulting in a 20 cm distance between the medial sides of the heels and 9° outward rotation of the feet with respect to the sagittal midline. The subjects faced a visual scene (4.80 × 3.70 m at a distance of 3.20 m) consisting of a light gray background.

To measure the ground reaction forces of both legs, we manufactured a custom-made force plate that consisted of four dof load cells (ATI-Mini45SI-580-20), mounted in a rectangular configuration on an aluminum plate. Each load cell was covered with a rectangular aluminum plate with dimension of 15 × 17.5 cm. The foot frame ensured that each foot was placed solely on the cover of two force sensors. The force plates were integrated in a top plate that was built on the Stewart Platform. Forces and torques of each load cell were sampled at a frequency of 360 Hz.

Reflective spherical markers were attached to heel, toe, malleolus, tibia, knee, femur, of both legs as well as the sacrum, head, and shoulders. In addition, a cluster of three markers was attached to the

[1] A Stewart motion platform, also known as a hexapod positioner, is a kind of parallel manipulator using an octahedral assembly of struts. A Stewart platform has 6 df (*x, y, z,* pitch, roll, and yaw).

anterior superior iliac spine of both legs and three markers were attached to the platform. The positions of the markers were recorded at a sample rate of 120 Hz by means of a three-dimensional passive motion capture system, consisting of six video cameras and a control unit (VICON). Body length and weight were measured for each subject.

The harness prevented the subjects from falling without constraining the movements necessary to maintain balance or providing any support or orientation information.

DATA PROCESSING. In the static trial, subjects were instructed to stand in anatomical position[2] for 10 s. From the recorded marker positions, the position of the CoM was calculated (Koopman et al. 1995). From the static trial, the height (l_{CoM}) of the CoM was determined as the average distance in the sagittal plane from the ankle to the CoM. The sway angle (θ) was calculated from l_{CoM} and the horizontal distance from the CoM to the mean position of the ankles. The platform displacement was reconstructed from the platform markers. The measured forces and torques from the four sensors were first resampled to a frequency of 120 Hz and subsequently corrected for the inertia and weight of the top cover similar as done by others (Preuss and Fung 2004). The corrected forces and torques from both sensors below each foot were used to calculate the vertical and horizontal forces acting on each foot and their point of application, being the CoP. The ankle torque was calculated using the CoP and the ground reaction forces (van der Kooij et al. 2005).

PROCEDURES. Subjects were instructed to "maintain their balance without moving their feet" while the continuous random platform movements were applied in the forward-backward direction. Before data recording, the perturbation was presented to the subject to become acquainted to the signal to minimize any transient behavior due to learning. The subjects had either their eyes open (EO) or eyes closed (EC). The amplitude of the platform motion (x_{sb}) was 6 or 8 cm for EO (EO6 and EO8) and 6 cm for EC (EC6). The RMS of the perturbation (d) magnitude was in the range of 28–56 and 50–100 Nm for the 6- and 8-cm platform motion amplitude, respectively. The order of the conditions was randomized. Before the platform perturbation onset, spontaneous sway was recorded during quiet standing for 180 s with eyes open (QS EO) and eyes closed (QS EC). Trials in which balance was lost, i.e., a stepping response or swinging of the arms, were repeated.

The mechanical perturbation of the platform movement is proportional to its acceleration. The magnitude of the perturbation further depends on the mass of the subject and the distance from the ankles to the CoM (van der Kooij et al. 2005)

$$d = -m_{CoM} I_{CoM} \ddot{x}_{sb} \quad (1)$$

where d is the external perturbation torque acting around the ankle, *[umlaut]*x_{sb} the forward-backward acceleration of the support base, l_{CoM}, the distance from the ankles to the CoM, and m_{CoM}, the mass of the subject.

PERTURBATION SIGNAL DESIGN. The perturbation signal was designed as a sum of sinusoids, referred to as a multisine signal. A multisine signal has several advantages(de Vlugt et al. 2003): it is periodic, which improves the estimation of FRFs; its power can be specified at any desired frequency' and when many different sinusoids are summated humans cannot predicted the signal, preventing effective feed forward control. The chosen multisine had a period of 34.13 s (equal to 2^{12} = 4,096 samples at a sample rate of 120 Hz) and contained power in the range of 0.06–4.4 Hz. To improve the NSR at the excited frequencies four frequency bands were not excited: 2.40–2.61, 2.87–3.08, 3.34–3.54, and 3.78–4.02 Hz. The power spectrum decreased logarithmically with frequency to obtain a flat spectrum for the acceleration. The power of the signal at a given amplitude was optimized by crest optimization (Schoukens et al. 1993). The perturbations were applied in two trials of 180 s for each condition. Each trial thus contained five whole perturbation cycles. The first 9.35 s of each trial was not used for data analysis to allow transient responses to decay. In total, for each subject and perturbation condition 10 blocks (M = 10) of data were collected.

[2] In the anatomical position, a subject is standing in a erect position with the palms of the hands facing forward and with the eyes and the ears in a horizontal plane.

Analysis

NONPARAMETRIC IDENTIFICATION. The goal of the nonparametric identification was to estimate the dynamics of the mechanisms that stabilize balance: $C(\omega)$, with ω the frequency in radians per second. The FRFs were estimated using standard frequency domain identification methods at the applied frequencies (Pintelon and Schoukens 2001). The periodic component is the invariant part of the response to equal perturbations, which was obtained by averaging over the repetitions

$$U_p(\omega) = \frac{1}{m}\sum_{l=1}^{m} U^l(\omega) \quad (2)$$

Where $U_p(\omega)$is the periodic part, $U^l(\omega)$ is the Fourier transform of signal $u(t)$ in the lth cycle (sway angle or ankle torque), and m the number of repetitions. The nonperiodic component is different for each cycle and is obtained from

$$U_n^l(\omega) = U^l(\omega) - U_p(\omega) \quad (3)$$

From the periodic components, the dynamics of the stabilizing controller were estimated. For this purpose, the body sway angle and ankle torque must be expressed as functions of all independent inputs (see Fig. 1)

$$T(\omega) = \frac{C(\omega)}{1 + C(\omega)P(\omega)} V(\omega) - \frac{C(\omega)P(\omega)}{1 + C(\omega)P(\omega)} D(\omega) - \frac{C(\omega)}{1 + C(\omega)P(\omega)} W(\omega) + M_2(\omega) \quad (4)$$

$$\theta(\omega) = \frac{C(\omega)P(\omega)}{1 + C(\omega)P(\omega)} V(\omega) + \frac{P(\omega)}{1 + C(\omega)P(\omega)} D(\omega) + \frac{1}{1 + C(\omega)P(\omega)} W(\omega) + M_3(\omega) \quad (5)$$

In which $C(\omega)$ is the FRF describing the stabilizing mechanisms, $P(\omega)$ the FRF of the body dynamics as simplified by an inverted pendulum, $V(\omega)$ the sensor noise, $D(\omega)$ the external perturbation, $W(\omega)$ the (unmeasured) output disturbance, and $M_2(\omega)$ and $M_3(\omega)$ are both measurement noise. The sensor noise can also be used to model slow fluctuations in the reference signal (Dijkstra 2000). Note that in the inverted pendulum model, $W(\omega)$ represents the effect of those forces that influence the CoM other than the external perturbations and the ankle torque. Model errors are also captured by $W(\omega)$ in case the body does not act as in inverted pendulum but as a multi-body.

When only the external perturbation contains a periodic component, the periodic ankle torque (*Eq. 4*) and the body sway angle (*Eq. 5*) are given by

$$T_p(\omega) = -\frac{C(\omega)P(\omega)}{1 + C(\omega)P(\omega)} D_p(\omega) \quad (6)$$

$$\theta_p(\omega) = \frac{P(\omega)}{1 + C(\omega)P(\omega)} D_p(\omega) \quad (7)$$

An estimate of the stabilizing dynamics, $C(\omega)$, can now be obtained

$$\hat{C}(\omega) = -\frac{T_p(\omega)}{\theta_p(\omega)} \tag{8}$$

An indication of the accuracy of the estimated FRF is given by the variance of $\hat{C}(\omega)$, being (Pintelon and Schoukens 2001)

$$\sigma^2_{\hat{C}}(\omega) = \frac{|\hat{C}(\omega)|^2}{m}\left(\frac{\sigma^2_{T_n}(\omega)}{|T_p(\omega)|^2} + \frac{\sigma^2_{\theta_n}(\omega)}{|\theta_p(\omega)|^2} - 2Re\left(\frac{\sigma^2_{T_n\theta_n}(\omega)}{T_p(\omega)\theta_p(\omega)}\right)\right) \tag{9}$$

Where $\sigma^2_{T_n}$ and $\sigma^2_{\theta_n}$ are the variances of the remnants (*Eq. 3*) of the ankle torque and $\sigma_{T_n\theta_n}$ is the cross-spectral density of the remnant parts of both signals, according to

$$\sigma^2_{T_n}(\omega) = \frac{1}{m-1}\sum_{l=1}^{m}|T^l_n|^2 \tag{10}$$

$$\sigma^2_{\theta_n}(\omega) = \frac{1}{m-1}\sum_{l=1}^{m}|\theta^l_n(\omega)|^2 \tag{11}$$

$$\sigma^2_{T_n\theta_n}(\omega) = \frac{1}{m-1}\sum_{l=1}^{m}\left(T^l_n(\omega)\right)\left(\overline{\theta^l_n(\omega)}\right) \tag{12}$$

The over-bar in *Eq. 12* denotes the complex conjugate.

It is also possible that the actual perturbation signal is not perfect periodic and contains a stochastic component. The remnant of the platform perturbation is

$$\sigma^2_{D_n}(\omega) = \frac{1}{m-1}\sum_{l=1}^{m}|D^1_n|^2 \tag{13}$$

The ratio of the remnant and periodic component is expressed by the NSR

$$NSR_T(\omega) = \frac{\sigma^2_{T_n}(\omega)}{|T_p(\omega)|^2} \tag{14}$$

$$NSR_\theta(\omega) = \frac{\sigma^2_{\theta_n}(\omega)}{|\theta_p(\omega)|^2} \tag{15}$$

In addition to the remnant magnitudes, the origin of the remnants was retrieved, discriminating between a stochastic source from outside the control loop (i.e., measurement noise) and a stochastic source that injects energy in the loop (i.e., sensory or output disturbance). The first step in the localization of remnants is to analyze the correlation between the body sway and ankle torque remnants. The correlation between the remnants of body sway and ankle torque is

$$\Gamma_{T_n\theta_n}(\omega) = \frac{\sigma^2_{T_n\theta_n}(\omega)}{\sqrt{\sigma^2_{T_n}(\omega)\sigma^2_{\theta_n}(\theta)}} \tag{16}$$

The expectation value for the correlation between body sway and ankle remnants can be found by substituting the *Eqs. 4* and *5* with only the nonperiodic components into *Eq. 16*. The resulting expression is given in APPENDIX from which the following conclusions can be drawn. *1*) The correlation function is a complex valued function. *2*) The magnitude of the correlation is always one or less than one. *3*) The correlation function depends on the noise variances $|M_2|^2$, $|M_3|^2$, $|V|^2$, $|W|^2$, $|D_n|^2$ and the system matrices P and C. *4*) $[\Gamma_{T_n}\theta_n]$ approaches zero in case measurement noise dominates, i.e.: $\{|M_2|^2, |M_3|^2\} \gg \{|V|^2, |W|^2, |D_n|^2\}$. *5*) The magnitude of $\Gamma_{T_n}\theta_n$ equals one only when one of the noise sources ($|V|^2$, $|W|^2$. $|D_n|^2$) dominate the other two and when the phase of $C(\omega)$ is zero.

From the correlation analysis, we found that for low frequencies the remnants are caused mainly by D_n, W, or V. D_n can be estimated directly from the data (*Eq. 13*) and appeared to be very small and could not explain the large body sway and ankle torque remnants. Consequently, the dominant sources of noise were W and/or V. The next step in the localization of remnants is the analysis of the ratio of the variances of ankle torque and body sway remnants. For the case in which we assume that $D_n = M_2 = M_3 = 0$, the ratio of the variances in ankle torque and body sway remnants can be found with *Eqs. 4*, *5*, *10*, and *11* and can be simplified into

$$\frac{\sigma^2_{T_n}(\omega)}{\sigma^2_{\theta_n}(\omega)} = \frac{|C|^2 f + |C|^2}{|C|^2|P|^2 f + 1} : f = \frac{|V|^2}{|W|^2} \tag{17}$$

We consider two extreme scenarios. First, for the output disturbance scenario we assumed that only output disturbance existed ($V = D_n = M_2 = M_3 = 0$). In this scenario, *Eq. 17* (with $f = 0$) equals the estimated controller dynamics

$$\frac{\sigma^2_{T_n}(\omega)}{\sigma^2_{\theta_n}(\omega)} = |C(\omega)|^2 \tag{18}$$

An estimate of the output disturbance can then be obtained from the estimated ankle torque remnant, according to *Eq. 4*

$$\sigma^2_W(\omega) = \left|\frac{1 + P(\omega)C(\omega)}{C(\omega)}\right|^2 \sigma^2_{T_n}(\omega) \tag{19}$$

or similarly from *Eq. 5*, from the body sway remnant

$$\sigma^2_W(\omega) = |1 + P(\omega)C(\omega)|^2 \sigma^2_{\theta_n}(\omega) \tag{20}$$

If the output disturbance assumption was true, then *Eqs. 19* and *20* should give similar results. In the second scenario, only sensor noise was assumed present. In this scenario, *Eq. 17* with f approaches infinity, the ratio of the ankle torque and body sway remnant equals the reciprocal of the body dynamics

$$\frac{\sigma^2_{T_n}(\omega)}{\sigma^2_{\theta_n}(\omega)} = \left|\frac{1}{P(\omega)}\right|^2 \tag{21}$$

From *Eqs. 4* and *5* and assuming the output disturbances, measurement noise, and nonperiodic components are zero, the sensor noise can be obtained from the estimated ankle torque remnant, being

$$\sigma^2_v(\omega) = \left|\frac{1 + P(\omega)C(\omega)}{C(\omega)}\right|^2 \sigma^2_{T_n}(\omega) \tag{22}$$

alternatively, from the estimated body sway remnant

$$\sigma^2_v(\omega) = \left|\frac{1 + P(\omega)C(\omega)}{P(\omega)C(\omega)}\right|^2 \sigma^2_{\theta_n}(\omega) \tag{23}$$

If the sensor noise assumption appeared to be true, then *Eqs. 22* and *23* should give similar results.

In summary: the correlation between body sway and ankle torque remnants can be used to discriminate between measurement noise and noise within the feedback loop and to check whether one stochastic source is dominant or not. Because the remnant of the perturbation can be directly estimated from the data, *Eqs. 4* and *5* can be used to evaluate how much of ankle torque and body sway remnants can be explained by the perturbation remnant. When the effects of measurement noise and perturbation remnant are negligible, the ratio of body and ankle torque remnants can be used to localize whether the stochastic source is on the input or on the output.

Model simulations

To investigate whether the estimated remnants, periodic components and FRFs are consistent with various concepts of human balance control, we derived models of those different concepts. To illustrate the properties of these different models, we simulated those models

with Matlab/Simulink (The Mathworks, Natick, MA). In the DISCUSSION, we will relate findings from those computer simulations to a theoretical analysis of those models that are available in literature. In the computer simulations, we applied the same perturbation signal as we applied to our human subjects. The RMS of the perturbation (*d*) magnitude was 15, 45, and 60 Nm for the small, medium, and large perturbation, respectively. The model predicted body sway and ankle torque was analyzed like the experimental data. The model (Fig. 2, *top left*) represents an inverted pendulum with a gravitational stiffness ($m_{CoM}gl_{CoM}$= 648 kgm^2/s2) and an inertia (J = 66 kgm^2). An intrinsic stiffness (K_i = 60 Nm/rad) was modeled, and a neural controller (*C*) with body sway and velocity as an input and a torque T_A as output. For the controller different concepts were modeled. *1*) Continuous LTI feedback controller with additive low-pass filtered noise (Fig. 2, *M1*). This model is comparable with Peterka's model (Peterka 2000). *2*) ON-OFF intermittent control (Fig. 2, *M2* and *M3*). This model is equivalent with the hypothesis of an open and closed loop region (Eurich and Milton 1996). When the body sway (velocity) is below threshold (off state) the position and/or velocity feedback is not effective, corresponding to open loop control. In case the thresholds are exceeded, the feedback channels will be effective (on state) and the model is in the closed loop region. The thresholds are twice as large in the large threshold model (Fig. 2, *M3*) than in the low-threshold model (Fig. 2, *M2*). *3*) Discrete control (Fig. 2, *M4*). In this case, the corrective torque does not change continuously but at discrete instances. This is modeled with a zero order hold circuit. In the model, T_A is only modified each 400 ms and kept constant in between. *4*) Impulsive bias control of compliant tendon (Fig. 2, *M5*). In this model, as postulated by Loram and colleagues (Loram et al. 2005a), the bias or offset of a compliant tendon is controlled in a discrete way. The time between bias adjustments is the "bias duration" (Loram et al. 2006). The zero order hold duration corresponds with a bias duration of 400 ms (Loram et al. 2006). It has been hypothesized that this bias duration reflects an intrinsic constraint of the neuromuscular control system (Loram et al. 2006). The tendon stiffness is 90% of the gravitational stiffness (K_t = 0.9 $m_{CoM}gl_{CoM}$) according to experimental estimates (Loram et al. 2005a). *5*) Impulsive bias control of mechano stretch reflex (Fig. 2 *M6* and *M7*). In this model, the bias or set point of a continuous delayed feedback loop with positional (k_p) and velocity (k_v) feedback gains. The model was evaluated with a small (K_{out} = 0.2, Fig. 2, *M6*) and high (K_{out} = 1, Fig. 2, *M7*) feedback gain of the outer feedback loop. The bias adjustments were also implemented with a zero order hold of 400 ms. *6*) ON-OFF intermittent control of mechano stretch reflex (Fig. 2, *M8* and *M9*). In this model, the bias of the continuous inner loop is only adjusted when the body sway angle exceeds its threshold, again with a small and high outer loop feedback gain.

All feedback gains in the inner and outer loops were chosen in such a way that the positional and velocity loop gain was similar for the different concepts. The positional loop gain was 600 Nm/rad and the velocity 350 Nms/rad. In all cases, the neural time delay was 100 ms.

RESULTS

Periodic responses and remnants

The power spectral densities (PSD) of periodic ankle torque responses ($|T_p(\omega)|^2$) for the different subjects for the EO8 condition are shown in Fig. 3. The power decreases with frequency. At the frequencies that are not excited (gray areas), the energy is smaller than at the neighboring frequencies. The PSD of the periodic ankle torque responses for EO6 en EC6 and the periodic body sway responses have a similar pattern (not shown).

The remnants PSD of the ankle torque ($\sigma^2_{T_n}(\omega)$) for EO8 are shown in Fig. 4. The energy decreases with frequencies. The PSD of ankle torque remnants for the other conditions and of the body sway remnants do have a similar pattern. The PSD of body sway and of ankle torque in QS also have this same pattern (results not shown).

The group means of the remnant PSD and PSD of the periodic responses at the excited frequencies were averaged within different frequencies bins, and the corresponding NSRs were determined (Fig. 5). The percentage of the responses that could be explained by its periodic component was calculated (Fig. 6) from the NSRs. In general, the NSR decreased with frequency. For the whole frequency range in which the perturbation was applied (0.06–4.5 Hz), the relative contri-

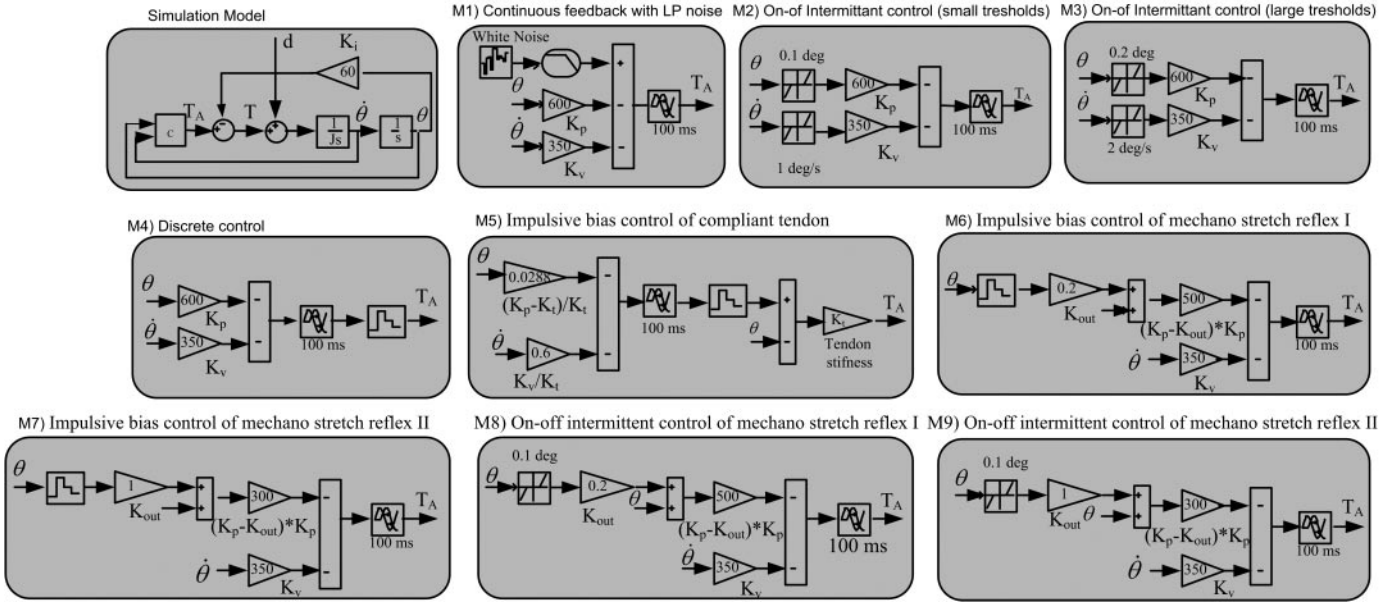

FIG. 2. General simulation model of balance control (*top left*) and 9 different models (*M1–M9*) representing the stabilizing mechanism as used to evaluate the experimental data.

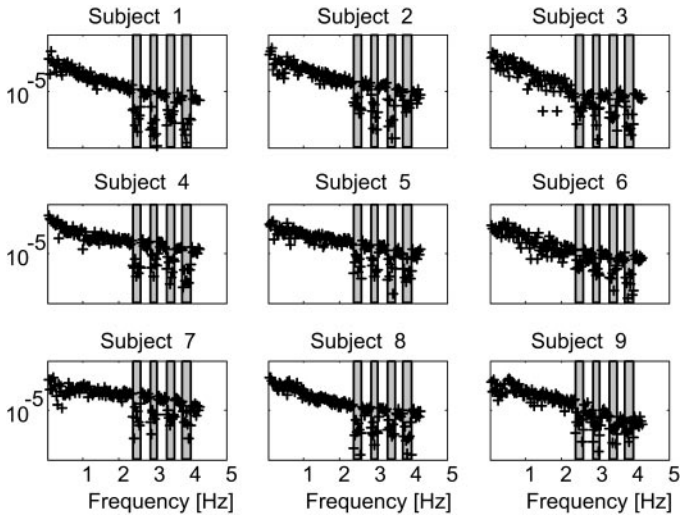

FIG. 3. Power spectral densities of the periodic ankle torque responses for EO8. Shaded areas show the frequencies where the perturbation signal contained zero power.

butions of the periodic responses was 82, 58, and 88% for body sway and 80, 75, and 86% for ankle torque during EO6, EC6, and EO8, respectively. Because the NSR decreased with frequency, the relative contribution increased when the slow responses were not considered. For the 0.2- to 4.5-Hz frequency range, >77% of body sway and >81% of ankle torque responses were periodic. For the 0.5- to 4.5-Hz frequency range, >90% of body sway and >85% of ankle torque responses were periodic.

EFFECT OF VISION. Differences between conditions were tested with a Student's *t*-test. Comparing perturbed standing with eyes closed (EC6) to eyes open (EO6), the periodic parts in the response of body sway $[|\theta_{p\theta}(\omega)|^2]$ for EC were smaller for frequencies <0.2 Hz and larger for frequencies >0.5 Hz (Fig. 5). For the ankle torque, the periodic parts $[|T_p(\omega)|^2]$ were larger >0.2 Hz during EC6 compared with EO6.

The remnant PSD of body sway ($\sigma^2_{\theta_n}(\omega)$) in EO6 was significant smaller than in EC6 for frequencies <1 Hz. The remnant PSD of ankle torque ($\sigma^2_{T_n}(\omega)$) in EO6 was significant smaller than in EC6 for all frequencies. No significant differences were found in the remnant PSD of ankle torque ($\sigma^2_{T_n}(\omega)$) and body sway ($\sigma^2_{\theta_n}(\omega)$) between QS EO and QS EC.

Compared with EO6, the NSR of body sway [$NSR_\theta(\omega)$] for EC6 was significant higher in the 0.06- to 1-Hz frequency range. The NSR of ankle torque [$NSR_T(\omega)$] was significant higher in EO6 than in EC6, except in the 0.2- to 0.5- and the 1- to 2-Hz frequency range.

EFFECT OF AMPLITUDE. For all frequency bins, periodic responses were significant larger for EO8 compared with EO6 for both ankle torque and body sway. The remnant PSD of ankle torque and body sway did not significantly change between EO6 and EO8. During quiet standing with eyes open (QS EO) the remnant PSD of body sway and ankle torque was significant smaller than of EO6 for all frequencies. The remnant PSD of body sway in EC6 was significant larger than in QS EC for frequencies <1 Hz. The remnant PSD of ankle torque in EC6 was significant larger than in QS EC for all frequencies.

The NSR of the body sway was significant smaller in EO8 compared with EO6 for all frequencies and for the ankle torque at frequencies <1 Hz.

Estimated deterministic feedback dynamics

The gain and phase of the estimated FRF from body sway to ankle torque are shown in Figs. 7 and 8, respectively. The gains were normalized to the gravitational stiffness ($m_{CoM}gl_{CoM}$). In general, the gain increased with frequency, which can be explained by derivative feedback (body sway velocity). However, in some subjects after an initial increase, the gain dropped for the highest frequencies (*subjects 3, 6,* and *9*). The maximal gain varied between subjects from three to nine. In general, the estimated phase was zero at the lowest frequency, increased with frequency and started to decrease from ~0.9 Hz. For some subjects, the phase lag decreased again at the highest frequencies (*subjects 1, 3, 6, 8,* and *9*). The maximal phase lead was ~20° and the maximal phase lag varied between subjects from −50 to −180°. The gain and phase did not significantly change between EO6 and EO8, except for subject 6. Gain and phase were dependent on the visual condition. The gain was significantly larger for EC6 than for EO6. Because for frequencies <1 Hz the phase shift from body sway to ankle torque is positive and most of the energy of the responses was <1 Hz (Fig. 3), ankle moment preceded body sway.

Analysis of remnants

The remnants of the ankle torque and body sway showed a high and negative correlation of minus one for low frequencies. The magnitude of the correlation was one for frequencies <1 Hz (Fig. 9). From this, we can conclude that the effect of measurement noise is negligible. Because the

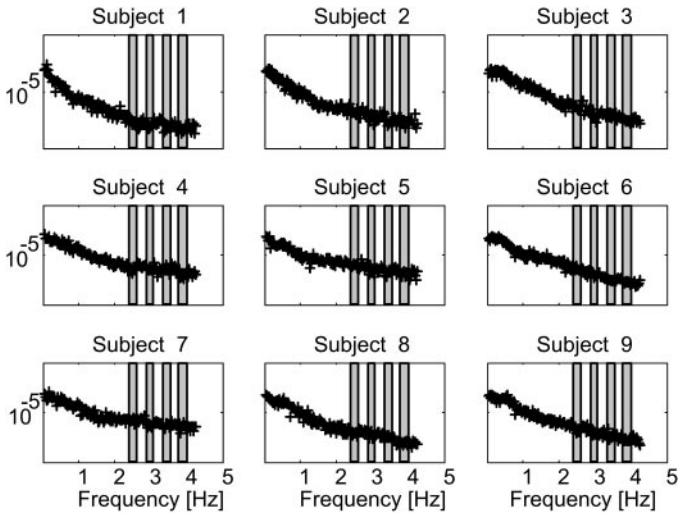

FIG. 4. The remnants of the ankle torque for EO8. Shaded areas show the frequencies where the perturbation signal contained zero power.

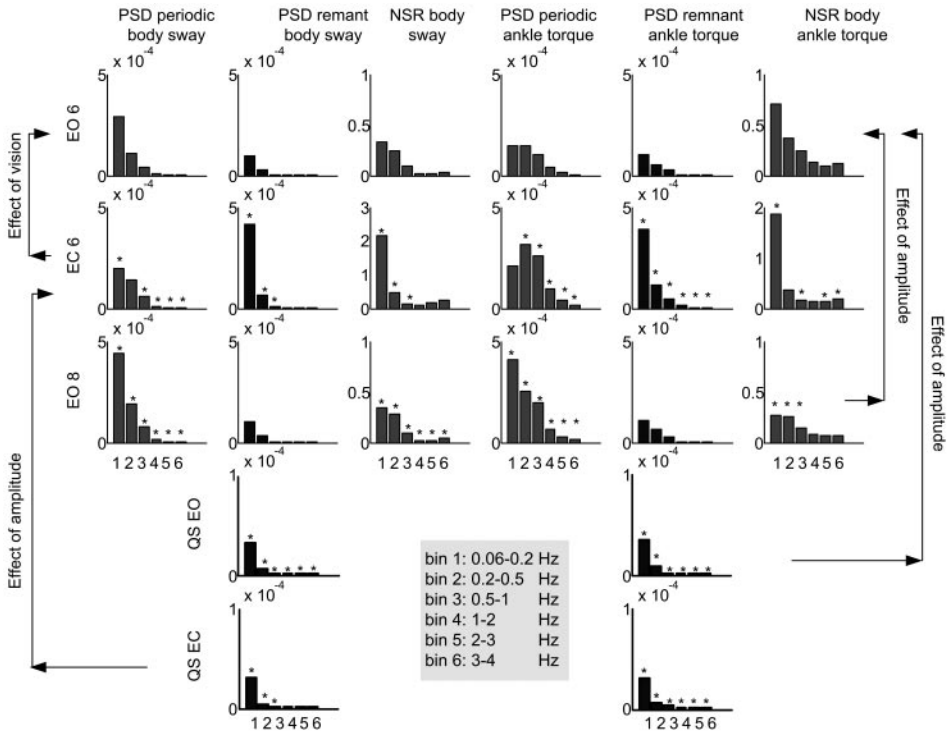

FIG. 5. Group mean of averaged power of the periodic (*1st column*) and remnant (*2nd column*) component of body sway and the corresponding noise-to-signal ratio (NSR, *3rd column*), and the power of the periodic (*4th column*) and stochastic component (*5th column*) of the normalized ankle torque, and the corresponding NSR (*6th column*). The power was averaged within 6 frequency bins. The power is shown for the conditions: eyes open 6 cm (EO6, *1st row*), eyes closed 6 cm (EC6, *2nd row*), EO 8 cm (EO8, *3rd row*), quite standing EO (QSEO, *4th row*), and QS EC (*5th row*). Stars denote significant ($P < 0.05$) differences between: EO6 and EC6 (*A*), EO6 and EO8 (*B*), EO6 and QSEO (*C*), or EC6 and QSEC (*D*). Note that the scale for QS and EO is different from scale for the perturbation trials.

perturbations remnants were very small (results not shown) we can also conclude that the stochastic source at the input dominates the stochastic source at the output (sensor noise scenario) or visa versa (output disturbance scenario).

OUTPUT DISTURBANCE SCENARIO. In the output disturbance model, it was assumed that there was only a stochastic output disturbance, together with the periodic external perturbation. Based on this assumption, the output disturbance $[\sigma^2_W(\omega)]$ was estimated (Fig. 10, *top left*) from the remnant PSD of body sway ($\sigma^2_{\theta_n}(\omega)$, see *Eq. 20*) and ankle torque ($\sigma^2_{T_n}(\omega)$, see *Eq. 19*). Using *Eq. 18,* the remnant PSD of body sway ($(\sigma^2_{T_n}(\omega))$ was calculated from the estimated ankle torque remnant PSD ($\sigma^2_{T_n}$) and the estimated FRF $[|\hat{C}(\omega)|]$ of the controller dynamics and compared with the directly estimated body sway remnant PSD (Fig. 10, *top middle*) and a similar comparison was performed for the remnant PSD of the ankle torque (Fig. 10, *top right*). For *subject 1,* the estimated output disturbance $[\sigma^2_W(\omega)]$ depended on whether it was estimated from the body sway remnant PSD or from the ankle torque remnant PSD (Fig. 10, *top left*). The predicted remnant PSD of the output disturbance model was different from the directly estimated remnant PSDs (Fig. 10, *middle* and *top right*).

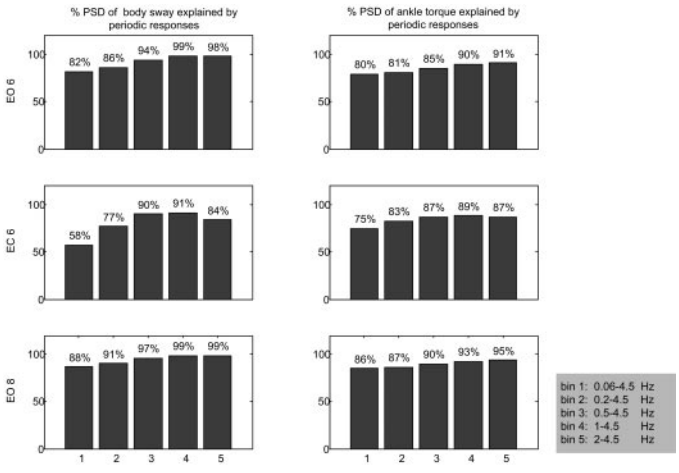

FIG. 6. Relative contribution of the periodic body sway (*left*) and ankle torque (*right*) for EO6 (*top*), EC6 (*middle*), and EO8 (*bottom*) clustered in frequency bins.

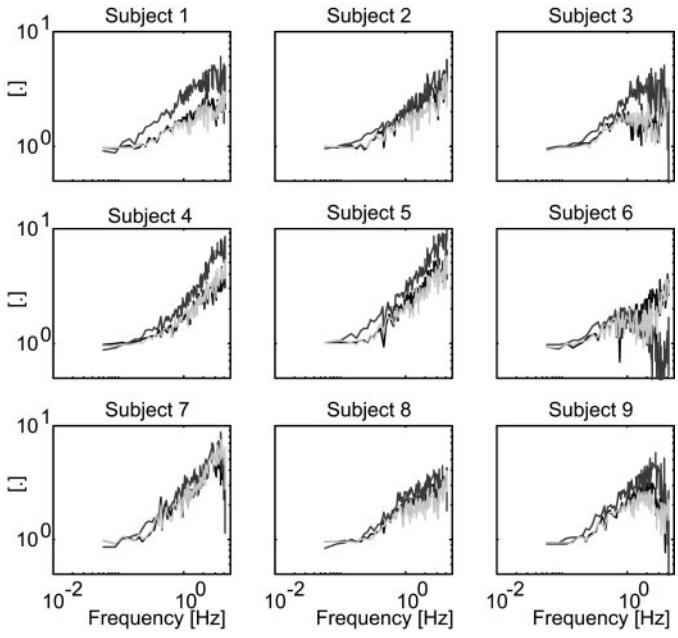

FIG. 7. Normalized gain of the estimated frequency response function (FRF) of the stabilizing ankle mechanism for EO6 (black lines), EC6 (dark gray lines), and EO8 (light gray lines) for all subjects.

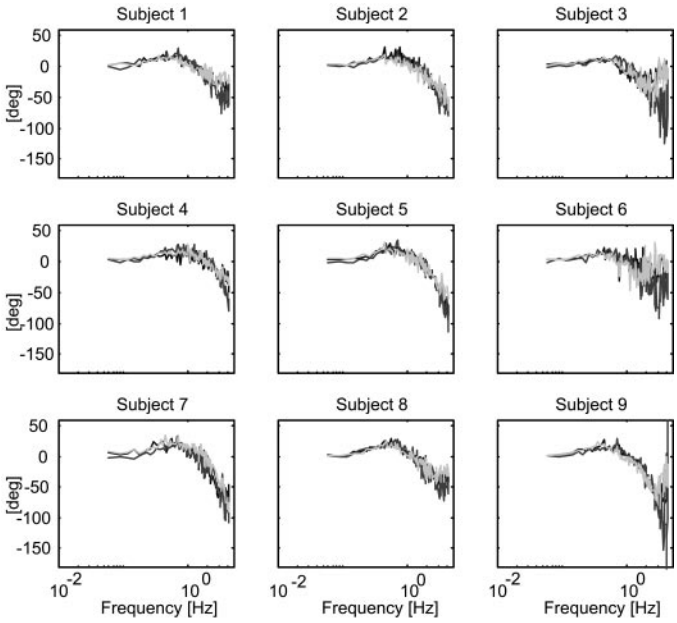

FIG. 8. Phase of the estimated FRF of the stabilizing ankle mechanism for EO6 (black lines), EC6 (dark gray lines), and EO8 (light gray lines) for all subjects.

Sensor noise scenario

In the sensor noise model, it was assumed that there is only sensor, or reference, noise together with the periodic external perturbation. Based on this assumption, the sensor noise [$\sigma_v^2(\omega)$] was estimated (Fig. 10, *bottom left*) from the ankle torque ($\sigma_{T_n}^2(\omega)$, see *Eq. 22*) and the body sway remnant PSD ($\sigma_{\theta_n}^2(\omega)$, see *Eq. 23*). The body sway remnant PSD was calculated from the estimated ankle torque remnant PSD and the inverted pendulum model (*Eq. 21*) and compared with the directly estimated body sway remnant PSD (Fig. 10, *bottom middle*). A similar comparison was made for the ankle torque remnant PSD (Fig. 10, *bottom right*). For *subject 1,* the estimated sensor noise, as obtained from the body sway remnant PSD, was quite similar to the version obtained from the estimated torque remnant PSD for frequencies <1 Hz (Fig. 10, *bottom left*). In addition, for frequencies <1 Hz, the predicted remnant PSD of body sway and ankle torque were similar to the directly estimated remnant PSDs (*bottom middle* and *right* in Fig. 10).

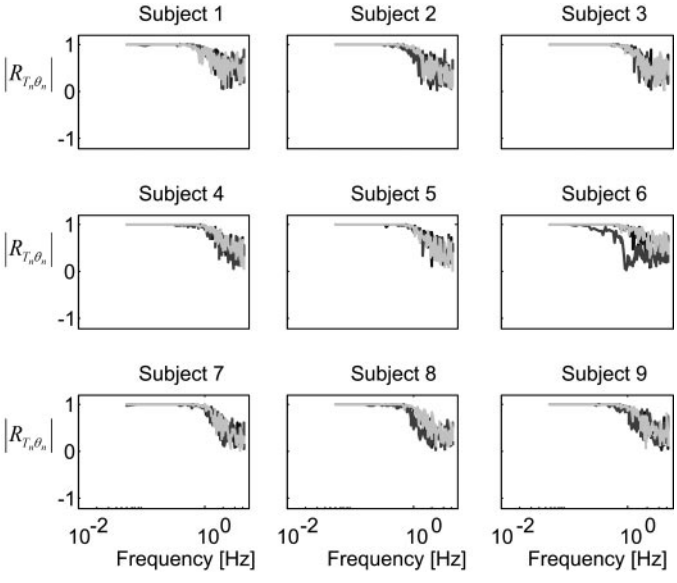

FIG. 9. Estimated correlations between normalized ankle torque and body sway remnants for EO6 (black lines), EC6 (dark gray lines), and EO8 (light gray lines) for all subjects.

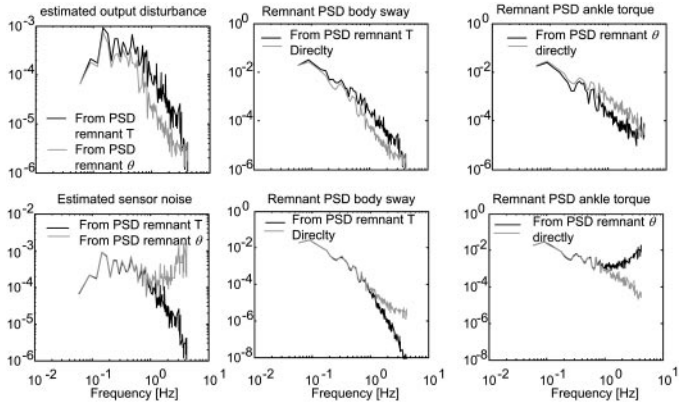

FIG. 10. Typical example (*subject 1,* EO6) of predictions of remnants according to the output disturbance scenario (*1st row*) and the sensor noise scenario (*2nd row*).

The ratio between the remnant PSD of ankle torque and body sway for frequencies <1 Hz corresponded well to the inverse pendulum model as predicted from the sensor noise scenario. The ratio did not resemble the estimated controller dynamics as predicted from the output disturbance scenario (Fig. 11).

From the characteristics shown in Figs. 10 and 11, it seemed that for frequencies <1 Hz, the ratio of body sway and torque remnant PSD is consistent with the sensor noise scenario.

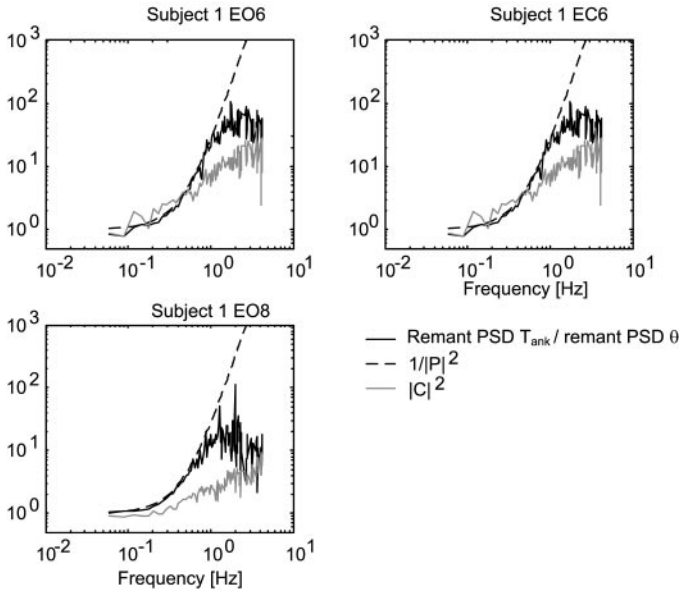

FIG. 11. Typical example (*subject 1*) of the ratio of the remnant PSD of the ankle torque and body sway (black solid lines) for EO6 (*top left*), EC6 (*top right*), and EO8 (*bottom left*). For the output disturbance scenario, the estimated ratio was determined by the squared modulus of the FRF of the stabilizing controller (solid gray lines). For the sensor noise scenario, the estimated ratio was determined by the reciprocal squared modulus of the FRF of the inverted pendulum model (dotted gray lines).

Similar as in Fig. 10 but for all subjects, the body sway remnant PSDs were determined from the ankle torque remnant PSDs, and visa versa, for both the output disturbance and the sensor noise scenarios for frequencies <1 Hz only (Fig. 12). For the output disturbance model, the differences between the directly estimated and indirectly computed remnants were significant for all frequency bins. For the sensor noise model, the differences were smaller than for the output disturbance model. For most frequency bins in eyes open conditions (EO6 and EO8), the differences were not significant.

Model simulations

The simulation results of the models (Fig. 2) were analyzed in a similar way as for the experimental results. The periodic components of the ankle torque are shown in Fig. 13. The remnants of the ankle torque for three perturbation amplitudes are shown in Fig. 14. The estimated gain and phases of the different controllers are shown in Fig. 15 and Fig. 16, respectively. We will summarize the results for the different models.

CONTINUOUS LTI FEEDBACK CONTROLLER WITH ADDITIVE LOW-PASS FILTERED NOISE (FIG. 2, *M1*). In the shape of the remnants, the low-pass filtered noise can be recognized (Fig. 14, *M1*). The periodic responses do have much less energy at the frequencies that are not excited (gray areas in Fig. 13) compared with the excited frequencies. The estimated gain increases with frequency and the estimated phase has no phase shift at lower frequencies, has a phase lead at medium frequencies and for higher frequencies has an increasing phase lag.

ON-OFF INTERMITTENT CONTROL (FIG. 2, *M2* AND *M3*). The remnants due to the stochastic nonlinear distortions have a similar shape as experimentally observed for some cases. The shape is dependent on the threshold and perturbation amplitude. For larger amplitudes, the remnants decrease, especially at lower frequencies. For a larger threshold, the remnants increase. The periodic responses and estimated gain and phases are similar to those for the continuous LTI feedback controller.

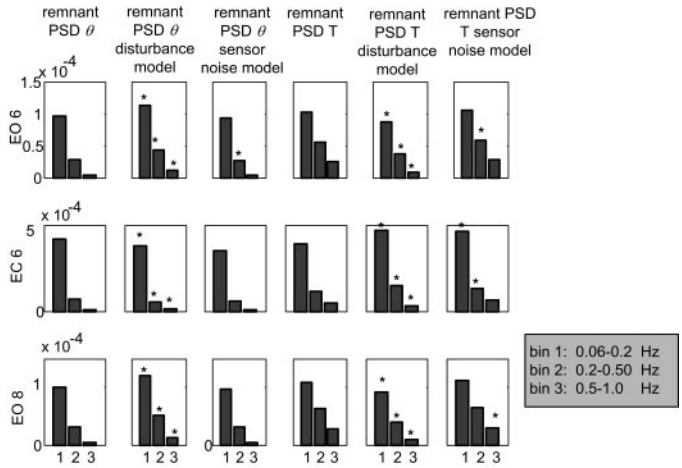

FIG. 12. Group mean of averaged remnant power spectral density (PSD) of body sway that were directly estimated (*1st column*), obtained from the output disturbance model (*2nd column*) and obtained from the sensor noise model (*3rd column*). Similar for the remnant PSD of the ankle torque (*4th, 5th,* and *6th columns*). The remnant PSDs were averaged within 3 frequency bins. The remnant PSDs are shown for the conditions EO6 (*1st row*), EC6 (*2nd row*), and EO8 (*3rd row*). Stars denote significant ($P < 0.05$) differences between the directly estimated remnant PSDs (*1st* and *4th columns*) and those obtained from the output disturbance or sensor noise.

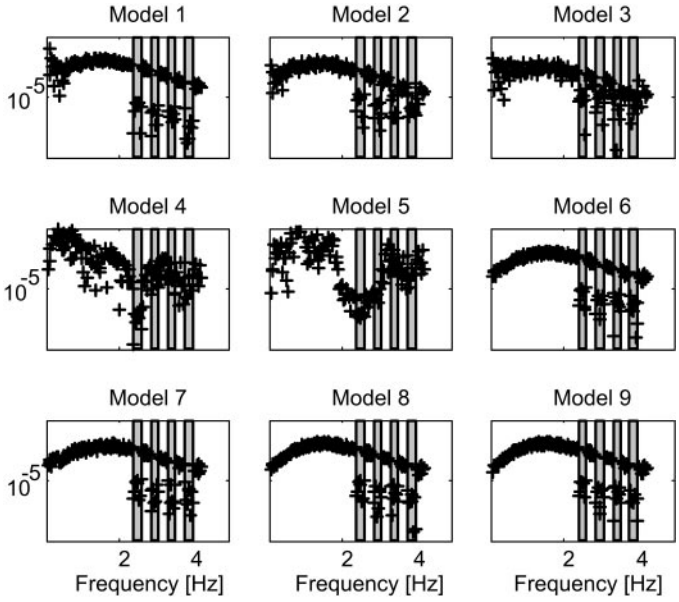

FIG. 13. PSDs of the periodic responses for the different modeled stabilizing mechanisms (see Fig. 2). Shaded areas show the frequencies where the perturbation signal contained no power.

DISCRETE CONTROL AND IMPULSIVE BIAS CONTROL (FIG. 2, *M4* AND *M5*). Drops in the PSD of the periodic components and remnants can be observed at the frequencies 1.25, 2.5, and 3.75 Hz. This frequency corresponds with the frequency and its higher harmonics at which the bias is adjusted or the control signal is updated [$f_d = 1/(2*0.4) = 1.25$ Hz]. The PSD of the periodic component also has considerable energy at those frequencies that were not excited (gray bands in Fig. 13). The shape of remnant PSD does not have the characteristic shape as experimentally observed in which most of the energy is concentrated at the lowest frequencies (Fig. 4).

NESTED CONTINUOUS INNER LOOP DISCONTINUOUS OUTER LOOP CONTROL (FIG. 2, *M6–M9*). The estimated gain and phase are similar to those estimated for the LTI feedback controller. Periodic responses at the nonexcited frequencies are negligible. The remnants were much smaller compared with all other cases.

DISCUSSION

Estimated responses are consistent with feedback control and noisy state estimation

The main goal of this study was to investigate whether the responses evoked by periodic perturbations can be explained by continuous time invariant feedback. In case of continuous time invariant deterministic feedback, the responses to periodic perturbations should be identical for each perturbation cycle. After applying a pseudo random periodic perturbation signal 10 times, the responses were divided into a periodic (deterministic) component and a nonperiodic (stochastic or remnant) component. The deterministic component is that part of the response that is similar each time the perturbation is applied. The remnant is the variation in the responses to repeated

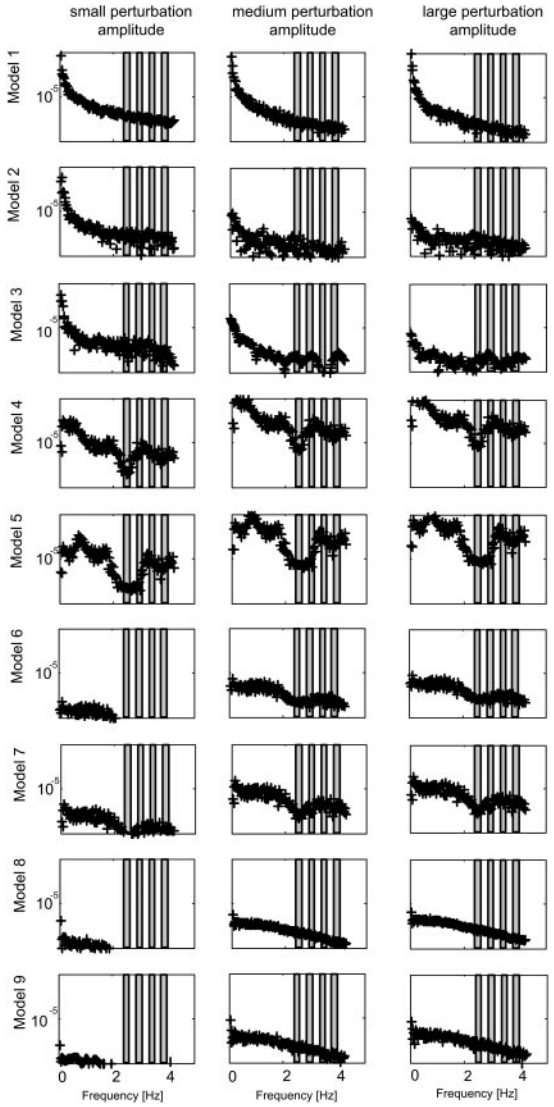

FIG. 14. Remnants for the different modeled stabilizing mechanisms (see Fig. 2) simulated with small, medium, and large perturbation amplitude. Shaded areas show the frequencies where the perturbation signal contained no power.

identical perturbations. Most of the measured responses were deterministic, especially at the higher frequencies. The deterministic responses are consistent with the idea that balance is controlled by continuous time invariant feedback. The FRFs of the feedback pathway were estimated. The phase lag dominated at higher frequencies, indicating the presence of delays that were most likely from neural transmission to and from the CNS. The remnants cannot be considered as a base line of spontaneous activity solely because the remnant PSD were significantly higher than the PSD of body sway and ankle torque during quiet standing.

The physiological cause of the remnants could be the imperfect processing of noisy sensory signals (Kiemel et al. 2002; van der Kooij et al. 1999), time variant behavior due to fatigue or adaptation, or to other discontinuous control mechanisms, which will be discussed in the next paragraph. Several results presented in this paper support the idea that the remnants are due to state estimation errors. First, most of the power of the remnant PSDs was at the lowest frequencies; this is consistent

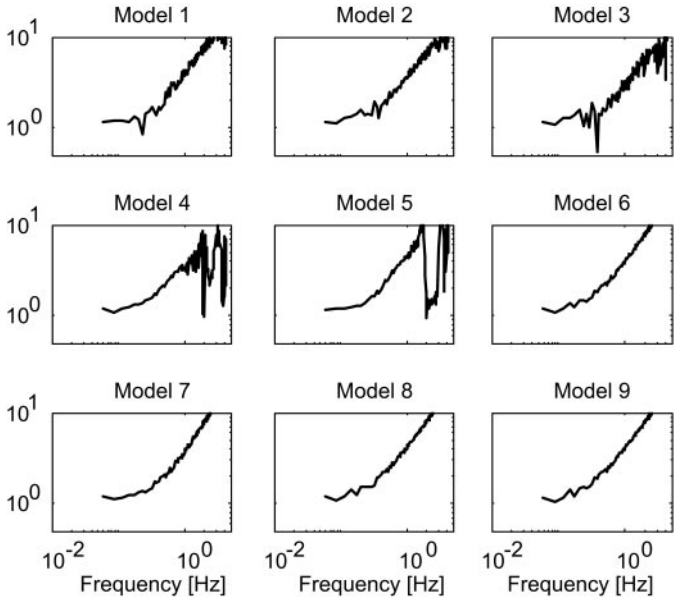

FIG. 15. Estimated gain for the different modeled stabilizing mechanisms (see Fig. 2).

with the claim that state computation noise is responsible for the slow dynamics that dominate spontaneous sway (Kiemel et al. 2002, 2005). Second, <1 Hz, the ratio of the remnant PSD of body sway and remnant PSD of ankle torque reflected the body dynamics; this is consistent with the idea that the remnants are due to estimation errors. Third, the remnants did increase when closing the eyes but did not increase when the perturbation amplitude was increased. Removing one source of sensory information increases state estimation errors (van der Kooij et al. 1999), whereas increasing the perturbation amplitude will not increase estimation errors, unless state-dependent noise exists. Therefore another important finding of this study is that the observed remnants of body sway and ankle torque supported the hypothesis that the dominant source of noise occurred *inside* the feedback loop.

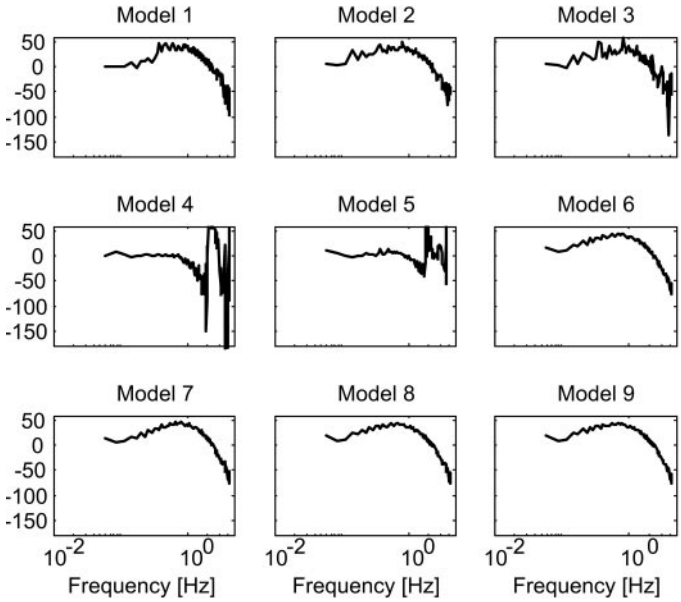

FIG. 16. Estimated phase for the different modeled stabilizing mechanisms (see Fig. 2).

In case of platform perturbations, the visual flow is not only related to body sway but also to the platform motion. During platform perturbations, visual information gives ambiguous clues about body orientation, unlike in quiet standing; the visual input not only depends on the body sway but also on the platform position and velocity. During the platform perturbation, the vestibular system also has to discriminate between forces acting on the otoliths that are caused by whole body accelerations or a change of the inclination vector of the body. In unperturbed standing, the change of forces on the otoliths can be attributed solely to changes in body inclination. The larger remnant PSD in perturbed conditions than the PSD of body sway and ankle torque during spontaneous sway can be understood from an increase in estimation errors because the sensory context during platform perturbations is more challenging compared with quiet standing. If the remnants are due to sensory integration errors, we hypothesize that *1*) the remnants will decrease for mechanical perturbations in which the visual and vestibular information only contains information of body motion and orientation and does not contain information of platform motion and acceleration. Pulling and pushing the body by a mechanical device is an example of such a perturbation (Fitzpatrick et al. 1992). *2*) The addition of sensory clues such as lightly touching a stable surface (Jeka and Lackner 1995; Lackner et al. 1999) will reduce the remnants.

(Contra) evidence for discontinuous stabilizing mechanisms?

FEED FORWARD CONTROL. Different researchers have argued that feedback is not the only mechanism that stabilizes balance but that feed forward or intermittent control is also involved. In this paragraph, we will critically review those claims and discuss whether the results presented in this paper are in conflict, or not, with alternative stabilizing mechanisms.

In the INTRODUCTION, we stated that feed forward control actions in principal can never contribute to stabilization because in its formal definition, the control variable is independent on the controlled variable. Fitzpatrick showed that body sway increased only with a factor two when the estimated neural feedback loop was removed from a model. Because this finding is in contrast with experimental results, he claimed that the neural system does not operate solely under feedback control and that possibly feed forward control strategies are utilized (Fitzpatrick et al. 1996). However, in their analysis it was not taken into account that the used formulas to calculate the PSD of body sway are only valid for a stable model. When the identified neural feedback loop was removed, the model was not stable anymore and the formulas used were no longer valid. In addition, the postulated alternative feed forward strategies were not true feed forward control schemes because the feed forward contribution was dependent on the body sway (Fig. 12B in Fitzpatrick et al. 1996). The proposed schemes have some similarities with disturbance compensation and adaptive feedback control, which are both feedback and not feed forward control.

Another proof of feed forward control was found in the observation that EMG leads the CoM (Gatev et al. 1999). However, an alternative definition of feed forward control was used in this paper: "by feed forward, we mean that the controller predicts an external input or behaves using high-order processing rather than simple negative feedback of a variable." Model simulations with a feedback model show that with combined position and velocity feedback the control variable leads the controlled variable (Fig. 16). Thus the phase advance of EMG over CoM motion can be due to CoM velocity feedback and does not necessarily imply other nonlinear predictive mechanisms. In addition, the phase advance was found with a cross-correlation analysis from unperturbed standing data. The results of this analysis are hard to interpret because observations from an unperturbed closed loop system cannot indicate causality (van der Kooij et al. 2005), and therefore it is impossible to state that the EMG causes a change in CoM or visa versa. Thus the relation between EMG and CoM does not necessarily reflect only the neural system but can also reflect the electromechanical delay, which could also explain why the EMG precedes body sway.

In conclusion, feed forward control has been used differently from its formal definition and evidence found for those feed forward mechanisms can be criticized. Because true feed forward control is not related to the output of the system and thus to the disturbance, feed forward contributions would appear in the remnants. The source of the remnants due to feed forward control would be at the input.

Intermittent control: bias adjustments

Averaging the responses in quiet standing revealed a pattern of ballistic-like throw and catch movements, which, according to the authors, was consistent with neural intermittent control (Loram and Lakie 2002). With elegant experimentation in a subsequent paper, they claimed that the calf muscles were controlled impulsively and ballistic (Loram et al. 2005b). The observed bias muscle adjustments were considered as a sign of intermittent alterations in neural output (Lakie and Loram 2006; Loram et al. 2006). On average, the unidirectional bias adjustments occurred at an interval of ~400 ms, which were considered as an intrinsic constraint of the neuromuscular system. From model simulation in which the bias of the tendon or the set point of a mechanoreceptor was adjusted each 400 ms, we learned that the power and gain of periodic responses dropped at the intermittent frequency of 1.25 Hz and its higher harmonics, 2.5 and 3.75 Hz. Those clear dips were not observed in our experimental results. In contrast with the experimental results, the model simulations showed comparable power at the nonexcited frequency bands as the neighboring excited frequencies. In addition, simulations with a linear time invariant feedback model driven by low-pass filtered noise showed that a throw-and-catch pattern in postural sway does not exclude continuous feedback control (Maurer and Peterka 2005b).

In conclusion, pure intermittent control reduces the gain of periodic responses at the intermittent frequencies and gives responses at those frequencies that are not excited, which we did not observe.

Intermittent control: open and closed loop region

The slow dynamics of postural sway can be explained by the existence of an open and closed loop region, which can be modeled by position and velocity thresholds (Eurich and Milton 1996). In the model simulations, the periodic responses and

the gain and phase of the estimated controller are similar to those of a continuous feedback controller and in corroboration with experimentally estimated periodic responses and the estimated controller dynamics. For some perturbation amplitudes, the remnants also have the same characteristic shape as experimentally observed. However, in the model simulations this characteristic shape of the remnants disappeared for large perturbation amplitudes. In contrast with experimental results, in the model, the remnants became smaller when the perturbation increased. The results in the model simulation are in line with a general theoretical framework that explains how thresholds result in slow fluctuations of postural sway but that the slow dynamics component disappears for larger perturbation amplitudes (Eurich and Milton 1996).

Although pure intermittent control is inconsistent with our experimental observations, we cannot rule out that intermittent control exists. Model simulations showed that in a nested control structure with a continuous inner loop and a discontinuous outer loop the periodic responses are similar to the responses of continuous feedback. When two or more models all agree with experimental results, standard scientific paradigm dictates that the preferred model is the one that is most parsimonious with assumptions at least until more evidence arrives to further constrain the models. From this perspective, the continuous feedback assumption is preferred because in the nested control loop structure, we assume that not only a continuous but also a discontinuous loop exists. In addition, in a nested control structure the characteristic of the remnants cannot be explained by the intermittent outer feedback loop.

Relation with other work

With a joint input-output identification the FRF of neural feedback pathways have been estimated (Fitzpatrick et al. 1996). The estimated phase increased with frequency $\leq 180°$ phase lead, whereas the estimated phase presented in this paper decreased at the higher frequencies and turned from a phase lead into a phase lag. We did identify the sum of intrinsic muscular and neural feedback pathways and not solely the neural feedback pathways. However, this cannot explain that we found a phase lag instead of phase lead at higher frequencies because intrinsic muscle properties act instantaneously and cannot produce phase lags. It would be interesting to reproduce the high phase lead around 180° at frequencies >3 Hz, which indeed is difficult to reconcile with neural feedback control.

We found that closing the eyes resulted in higher feedback gains (Fig. 7). The higher feedback gains resulted in a decrease of the low-frequency periodic body sway responses, an increase of the high-frequency periodic body responses and an increase of the higher frequency periodic ankle torque responses. This is in contrast with a related study that did not find difference in the estimated gain between EO and EC (Fitzpatrick et al. 1996) but is in agreement with studies that found an increase in gain when eyes were closed (Ishida et al. 1997; Werness and Anderson 1984). We found an increase in the remnants when closing the eyes, which is in agreement with a study that found a larger error to signal ratio in EC compared with EO (Johansson et al. 2001) and with a parametric identification of noise models for which the estimated noise levels were higher for EC compared with EO (Werness and Anderson 1984). We did not find an increase in remnants, whereas others found an increase in noise levels with perturbation amplitude (Werness and Anderson 1984). We also did not find an increase in feedback gains when the platform perturbation amplitude was increased, as found in a previous study (Park et al. 2004). In a comparable study, the feedback gains also did not increase when the platform perturbation was enhanced (Alexandrov et al. 2005). An explanation for the invariant feedback gains and remnants with perturbation amplitude could be that in the latter study as well as in ours, the alterations in perturbation amplitude were not large enough to require rescaling of feedback gains to stay within biomechanical constraints.

For some subjects the estimated gain normalized to the gravitational stiffness was smaller than one at the lowest frequencies. For these subjects, the estimated ankle feedback mechanisms alone were insufficient to guarantee stability in case of the inverted pendulum model. Although we only analyzed the ankle torque, this does not imply that we assumed the subjects to behave as an inverted pendulum. Interestingly, also the knee and hip eigenmovements that contribute to stability have a significant contribution to ankle torque (Alexandrov et al. 2005). For a correct stability analysis, the knee and hip torques should also be taken into account. The presented nonparametric identification method could be combined with the eigenmovement approach.

Other studies that identified the feedback pathway (Alexandrov et al. 2005; Barin 1989; Peterka 2002) used parametric methods to estimate the feedback pathway, whereas we used a nonparametric approach. The method we used is a direct identification method that will only work for periodic perturbations, which means that the NSR should be sufficiently small (Pintelon and Schoukens 2001). We found no differences with the estimated FRFs as obtained with the direct method or the joint input-output method, which is more robust for high NSRs (van der Kooij et al. 2005). We used continuous pseudorandom perturbation instead of transient perturbations (Alexandrov et al. 2005; Barin 1989; Park et al. 2004) because continuous perturbations contain more energy at higher frequencies (Kearney and Hunter 1990); the predictability of transient inputs might provoke the subject to learn the nature of the stimulus waveform, which may induce voluntary responses to the perturbation; and with continuous perturbations, the system is analyzed in its stationary functioning, whereas for transient perturbations, it could be well possible that the system is in transition from one stationary condition to the other. Because humans are very well capable to adapt their strategy when task or environment conditions change it is less likely that during a transient the system act as a linear time invariant system.

Balance control is a continuous nonlinear system that can be considered quasi linear in stationary conditions

The goal of this paper is to investigate whether the periodic components and the remnants of responses evoked by pseudorandom periodic platform perturbations are consistent with continuous feedback control or otherwise with alternative concepts of balance control as proposed by others. With model simulation, we showed that the evoked responses were consistent with continuous time invariant feedback control and that no indications of discontinuities were found. Because also the gain and phases and the remnants did not scale with the perturbation amplitude the feedback mechanisms could also be

considered linear, at least within the range of perturbations applied.

Can we conclude from these results that the postural control is linear and continuous for other experimental conditions than applied in this study? No we cannot.

In this study, we considered the dynamics from body sway motion to ankle torque. It is known that visual, vestibular, and proprioceptive feedback channels are part of these dynamics. It has been shown that the relative weight of the different channels depend on the visual and support base conditions (Peterka 2002). Peterka used system identification techniques similar as in this paper and considered balance control for a given stimulus amplitude as quasi linear. Note that in this study both the visual surround and support base rotations were constant. With similar system identification techniques, it has been shown how the postural control of the arm is highly adaptable to changes in the frequency spectrum of the perturbation (van der Helm et al. 2002), to external applied stiffness and damping (de Vlugt et al. 2002), and to the configuration of the arm (de Vlugt et al. 2006). So we know that balance control and postural control in itself is very adaptive to environmental conditions and even to cognitive factors like fear (Adkin et al. 2000). Nevertheless, in stationary conditions or a range of stationary conditions, the system can be considered quasi linear and the responses will not be effected by possible mode switching.

Because we know that the system is highly adaptable to environmental conditions, we cannot easily extrapolate the results to other conditions, like unperturbed standing. But previous work (Kiemel et al. 2002; Maurer and Peterka 2005a; Peterka 2000) showed that the structure of sway in unperturbed conditions can be well approximated by LTI models that are consistent with the model we used (Fig. 1). With the applied or similar system identification techniques, we can systematically change the environmental conditions and quantify how the system has been adapted from one condition to the other as for example Peterka did. To approximate the unperturbed conditions closer, smaller perturbations can be applied. We do not expect that for smaller perturbations amplitudes balance control will behave as an intermittent controller. However, experiments have to be done to see whether the characteristics of postural responses for smaller perturbations differ from the perturbations we applied in this study.

Although the system identification utilized techniques in this paper are well suited to quantify the system in stationary conditions and how the system has been adopted from one stationary conditions to the other, these techniques are not suited to estimate the adaptation dynamics; i.e., how (fast) the system adapts to a different conditions. To estimate the adaptation dynamics different techniques can be applied, like wavelet analysis.

Conclusion

Concepts found in literature that balance is controlled discontinuously or intermittently instead of continuously are not consistent with responses evoked by pseudo-random periodic platform perturbations. The found results are consistent with the concept that balance control is a continuously feedback mechanism in which variations in responses are due to noisy state estimation errors. A nested control structure with a continuous inner feedback loop and discontinuous outer feedback loop is also consistent with experimental data. However, this is only true when the inner continuous feedback loop dominates postural responses.

APPENDIX

Assuming that V, W, M_2, and M_3 are nonperiodic, the remnants of the ankle torque and body sway can be found from *Eqs. 4* and *5*

$$T_n(\omega) = \frac{C(\omega)}{1 + C(\omega)P(\omega)} V(\omega) - \frac{C(\omega)P(\omega)}{1 + C(\omega)P(\omega)} D_n(\omega) - \frac{C(\omega)}{1 + C(\omega)P(\omega)} W(\omega) + M_2(\omega) \quad (A1)$$

$$\theta_n(\omega) = \frac{C(\omega)P(\omega)}{1 + C(\omega)P(\omega)} V(\omega) + \frac{P(\omega)}{1 + C(\omega)P(\omega)} D_n(\omega) + \frac{1}{1 + C(\omega)P(\omega)} W(\omega) + M_3(\omega) \quad (A2)$$

The cross correlation function follows from substitution of *Eqs. A1* and *A2 into Eq. 16*

$$\Gamma_{T_n\theta_n}(\omega) = -\frac{|C|^2P||V|^2 + C|P|^2|D_n|^2 + C|W|^2}{\sqrt{|C|^4|P|^2|V|^4 + |C|^2|P|^4|D_n|^4 + |C|^2|W|^4 + R_2}} \quad (A3)$$

Since

$$P = \frac{1}{Js^2 - mgl} = -\frac{1}{J\omega^2 + mgl} = -|P| \quad (A4)$$

Equation A3 can be rewritten into

$$\Gamma_{T_n\theta_n}(\omega) = -\frac{|C|^2|P||V|^2 + C|P|^2|D_n|^2 + C|W|^2}{\sqrt{|C|^4|P|^2|V|^4 + |C|^2|P|^4|D_n|^4 + |C|^2|W|^4 + R_2}} \quad (A5)$$

where

$$\begin{aligned} R_2 = {} & |C|^2|P|^2|V|^2|D_n^2 + |C|^2|V|^2|W|^2 + |C|^2V^2|M_3|^2|1 + PC^2| + \ldots \\ & \ldots + |C|^4|P|^4|V|^2|D_n|^2 + |C|^2|P|^2|W|^2|D_n|^2 + |C|^2|P|^2|D_n|^2|M_3|^2|1 + PC|^2 + \ldots \\ & \ldots + |C|^4|P|^2|W|^2|V|^2 + |C|^2|P|^2|W|^2|D_n|^2 + |C|^2|W|^2|M_3|^2|1 + PC|^2 + \ldots \\ & \ldots + |C|^2|P|^2|M_2|^2|V|^2 + |P|^2|M_2|^2|D_n|^2 + |M_2|^2|W|^2|1 + PC|^2 \\ & + |M_2|^2|M_3|^2|1 + PC|^4 \end{aligned} \quad (A6)$$

From *Eqs. A5* and *A6* we can conclude that $\Gamma_{T_n}\theta_n(\omega)$ is a complex valued function. Its magnitude is smaller than one in case, R_2 contributes significantly to the denominator. R_2 does contribute significantly to the denominator when two or more noise sources levels are of the same order of magnitude or when the effect of measurement noise is in the same order of the effects of V, D_n, or W. In case the phase of C is different from zero, the magnitude of numerator of *Eq. A5* is smaller than the magnitude of the denominator even if $R_2 = 0$.

The cross-correlation of body sway and ankle torque remnants can thus only be one if the contributions of measurement noise in the body sway and ankle torque remnants are negligible, the phase of C is zero, and one of the noise sources V,W, or D_n dominates.

REFERENCES

Adkin AL, Frank JS, Carpenter MG, Peysar GW. Postural control is scaled to level of postural threat. *Gait Posture* 12: 87–93, 2000.

Alexandrov A, Frolov A, Horak F, Carlson-Kuhta P, Park S. Feedback equilibrium control during human standing. *Biol Cybern* 93: 309–322, 2005.

Barin K. Evaluation of a generalized model of human postural dynamics and control in the sagittal plane. *Biol Cybern* 61: 37–50, 1989.

Bottaro A, Casadio M, Morasso PG, Sanguineti V. Body sway during quiet standing: is it the residual chattering of an intermittent stabilization process? *Hum Mov Sci* 24: 588–615, 2005.

Carver S, Kiemel T, van der Kooij H, Jeka JJ. Comparing internal models of the dynamics of the visual environment. *Biol Cybern* 92: 147–163, 2005.

Collins JJ, De Luca CJ. Open-loop and closed-loop control of posture: a random-walk analysis of center-of-pressure trajectories. *Exp Brain Res* 95: 308–318, 1993.

de Vlugt E, Schouten AC, van der Helm FC. Adaptation of reflexive feedback during arm posture to different environments. *Biol Cybern* 87: 10–26, 2002.

de Vlugt E, Schouten AC, van der Helm FC. Closed-loop multivariable system identification for the characterization of the dynamic arm compliance using continuous force disturbances: a model study. *J Neurosci Methods* 122: 123–140, 2003.

de Vlugt E, Schouten AC, van der Helm FC. Quantification of intrinsic and reflexive properties during multijoint arm posture. *J Neurosci Methods* 155: 328–349, 2006.

Dijkstra T. A gentle introduction to the dynamic set-point model of human postural control during perturbed stance. *Hum Mov Sci* 19: 567–595, 2000.

Eurich CW, Milton JG. Noise-induced transitions in human postural sway. *Phys Rev E Stat Phys Plasmas Fluids Related Interdisciplinary Topics* 54: 6681–6684, 1996.

Fitzpatrick RC, Burke D, Gandevia C. Loop gain of reflexes controlling human standing measured with the use of postural and vestibular disturbances. *J Neurophysiol* 76: 3994–4008, 1996.

Fitzpatrick RC, Taylor JL, McCloskey DI. Ankle stiffness of standing humans in response to imperceptible perturbation: reflex and task-dependent components. *J Physiol* 454: 533–547, 1992.

Gatev P, Thomas S, Kepple T, Hallett M. Feedforward ankle strategy of balance during quiet stance in adults. *J Physiol* 514: 915–928, 1999.

Ishida A, Imai S, Fukuoka Y. Analysis of the posture control system under fixed and sway-referenced support conditions. *IEEE Trans Biomed Eng* 44: 331–336, 1997.

Jeka J, Lackner JR. The role of haptic cues from rough and slippery surfaces in human postural control. *Exp Brain Res* 103: 267–276, 1995.

Johansson R, Magnusson M, Akesson M. Identification of human postural dynamics. *IEEE Trans Biomed Eng* 35: 858–869, 1988.

Johansson R, Magnusson M, Fransson PA, Karlberg M. Multi-stimulus multi-response posturography. *Math Biosci* 174: 41–59, 2001.

Kearney RE, Hunter IW. System identification of human joint dynamics. *Crit Rev Biomed Eng* 18: 55–87, 1990.

Kiemel T, Oie K, Jeka JJ. Multisensory fusion and the stochastic structure of postural sway. *Biol Cybern* 87: 262–277, 2002.

Kiemel T, Oie KS, Jeka JJ. The slow dynamics of postural sway are in the feedback loop. *J Neurophysiol* 95: 1410–1418, 2006.

Koopman B, Grootenboer HJ, de Jongh HJ. An inverse dynamics model for the analysis, reconstruction and prediction of bipedal walking. *J Biomech* 28: 1369–1376, 1995.

Lackner JR, DiZio P, Jeka J, Horak FB, Krebs DE, Rabin E. Precision contact of the fingertip reduces postural sway of individuals with bilateral vestibular loss. *Exp Brain Res* 126: 459–466, 1999.

Lakie M, Loram ID. Manually controlled human balancing using visual, vestibular and proprioceptive senses involves a common, low frequency neural process. *J Physiol* 577: 403–416, 2006.

Loram ID, Gawthrop P, Lakie M. The frequency of human, manual adjustments in balancing an inverted pendulum is constrained by intrinsic physiological factors. *J Physiol* 577: 417–432, 2006.

Loram ID, Lakie M. Human balancing of an inverted pendulum: position control by small, ballistic-like, throw and catch movements. *J Physiol* 540: 1111–1124, 2002.

Loram ID, Maganaris CN, Lakie M. Active, non-spring-like muscle movements in human postural sway: how might paradoxical changes in muscle length be produced? *J Physiol* 564: 281–293, 2005a.

Loram ID, Maganaris CN, Lakie M. Human postural sway results from frequent, ballistic bias impulses by soleus and gastrocnemius. *J Physiol* 564: 295–311, 2005b.

Maurer C, Peterka RJ. A new interpretation of spontaneous sway measures based on a simple mode. *J Neurophysiol* 93: 189–200, 2005a.

Maurer C, Peterka RJ. A throw-and-catch pattern in postural sway does not exclude continuous feedback control (Abstract). *Gait Posture* 21: S140, 2005b.

Mergner T, Maurer C, Peterka RJ. A multisensory posture control model of human upright stance. *Prog Brain Res* 142: 189–201, 2003.

Park S, Horak FB, Kuo AD. Postural feedback responses scale with biomechanical constraints in human standing. *Exp Brain Res* 154: 417–427, 2004.

Peterka RJ. Postural control model interpretation of stabilogram diffusion analysis. *Biol Cybern* 82: 335–343, 2000.

Peterka RJ. Sensorimotor integration in human postural control. *J Neurophysiol* 88: 1097–1118, 2002.

Peterka RJ. Simplifying the complexities of maintaining balance insights provided by simple closed-loop models of human postural control. *IEEE Eng Med Biol Mag* 22: 63–68, 2003.

Pintelon R, Schoukens J. *System Identification: A Frequency Domain Appoach*. New York: IEEE Press, 2001.

Preuss R, Fung J. A simple method to estimate force plate inertial components in a moving surface. *J Biomech* 37: 1177–1180, 2004.

Schoukens J, Guillaume P, Pintelon R. Design of broadband excitation signals. In: *Perturbation Signals for System Identification*, edited by Godfrey KR. Englewood Cliffs, NJ: Prentice Hall, 1993.

van der Helm FC, Schouten AC, de Vlugt E, Brouwn GG. Identification of intrinsic and reflexive components of human arm dynamics during postural control. *J Neurosci Methods* 119: 1–14, 2002.

van der Kooij H, Jacobs R, Koopman B, Grootenboer H. A multisensory integration model of human stance control. *Biol Cybern* 80: 299–308, 1999.

van der Kooij H, van Asseldonk E, van der Helm FC. Comparison of different methods to identify and quantify balance control. *J Neurosci Methods* 145: 175–203, 2005.

Werness SA, Anderson DJ. Parametric analysis of dynamic postural responses. *Biol Cybern* 51: 155–168, 1984.